JCSE The Journal of Corrosion Science and Engineering

ISSN 1466-8858

Volume 10 Paper 24

An Investigation of Corrosion Inhibitor – Iron Carbonate Scale Interaction in Carbon Dioxide Corrosion

K. Chokshi, W. Sun, and S. Nešić*
*Institute for Corrosion and Multiphase Technology, Department of Chemical and Biomolecular Engineering, Ohio University, Athens, OH 45701, USA. * Corresponding author: nesic@ohio.edu*

Abstract

An investigation was conducted on the interaction between corrosion inhibition and a precipitating iron carbonate scale, and their combined effects on the carbon dioxide corrosion rate. Both the effects of iron carbonate precipitation on inhibition and vice versa were studied using electrochemical techniques. The experiments were performed in a glass cell at 80 °C and an iron carbonate supersaturation range of 7 – 150. A generic imidazoline based inhibitor was added at various points in the iron carbonate scale formation process. The scale was later analyzed using scanning electron microscopy (SEM). Although no antagonism was found under any condition tested, it was observed that the addition of the inhibitor which hindered the corrosion rate, has retarded the growth of the iron carbonate scale by lowering the concentration of ferrous ion on the steel surface.

Keywords: iron carbonate, scale, inhibitor, precipitation, carbon dioxide corrosion

Introduction

Carbon dioxide corrosion is a major problem in the oil and gas industry and can occur at all stages of production from downhole to surface equipment (ref1). Although there have been many developments in corrosion resistant alloys over the past few decades, mild steel still constitutes an estimated 99% of the material used in the oil industry. The corrosion resistance of mild steel is poor in the aggressive environments, and the cost savings can only be realized by adding a corrosion inhibitor to the environment or applying a protective coating to the steel (ref2).

In carbon dioxide corrosion, iron carbide (ref1 and ref2) or iron carbonate scale (ref3 - ref10) may form on the surface due to the corrosion process. As a result, the surface of the metal is not always bare when the inhibitor is applied. Depending on the time when the inhibitor is added, the presence of the corrosion scale could affect the workings of the inhibitor. However very little research has been devoted to study of corrosion inhibition of the steel covered with corrosion product layers.

Gulbrandsen (ref1) et al. observed that inhibitor performance was impaired with increasing precorrosion time and increasing temperature. The inhibitor problems were attributed to the presence of the iron carbide layer at the steel surface. The longer the precorrosion time, the thicker the iron carbide scale would grow and more severely the inhibitor performance was impaired. However, the failure of the inhibitor was not due to transportation of the inhibitor to the metal surface. One reason cited for inhibitor failure was that the high metal dissolution rates prevented the slowly adsorbing inhibitors from attaching onto the metal surface and protecting it from corrosion. This phenomenon is described by the electromechanical inhibitor desorption model of V. Drazic and D. Drazic (ref11). Nesic (ref12) et al. observed that in the presence of iron carbide as well as iron carbonate scale the performance of an imidazoline-based inhibitor was very

poor. They concluded that it was the changes on the steel surface due to the precorrosion, which was responsible for the weaker performance of the inhibitor rather than the scale itself acting as a diffusion barrier for the inhibitor. Malik (ref13) investigated the effect of an amine based inhibitor on the surface scales. He found that in the presence of iron carbonate scale, lower concentrations of inhibitor seemed to work better than the higher concentrations. He also found that in the presence of inhibitor, there was a transformation of the surface structure of iron carbonate. However, the experiments were performed at room temperature, where the precipitation rate of iron carbonate is very slow. Therefore, the surface of the metal would have been predominantly covered by iron carbide scales rather than iron carbonate scales.

From the preceding discussion, a lack of understanding regarding the interaction between the iron carbonate scale and inhibitor is evident. The objective of the present work was to investigate

- the effect of corrosion inhibition on the growth of iron carbonate scale,
- the effect of iron carbonate scale on the performance of the inhibitor, and
- their combined effect on the corrosion rate.

Experimental Procedure

The experiments were done in a glass cell, as shown in Figure 1. A saturated Ag/AgCl reference electrode used externally was connected to the cell via a Luggin capillary and a porous wooden plug. A concentric platinum ring was used as a counter electrode. Each glass cell was filled with 2 liters of distilled water and 1% wt. NaCl. The solution was then heated to 80^{o}C and purged with CO_2 gas. After the solution was deoxygenated, the pH was increased from the equilibrium pH 4.18 to the desired pH by adding a deoxygenated sodium bicarbonate solution. Later the required amounts of Fe^{2+} were added in the form of a deoxygenated ferrous chloride salt ($FeCl_2$.4H2O) solution. Then the working electrode was inserted into the solution

and the measurements were taken. Prior to immersion, the mild steel specimen surfaces were polished with 240, 400 and 600 grit SiC paper in succession, rinsed with alcohol and degreased using acetone.

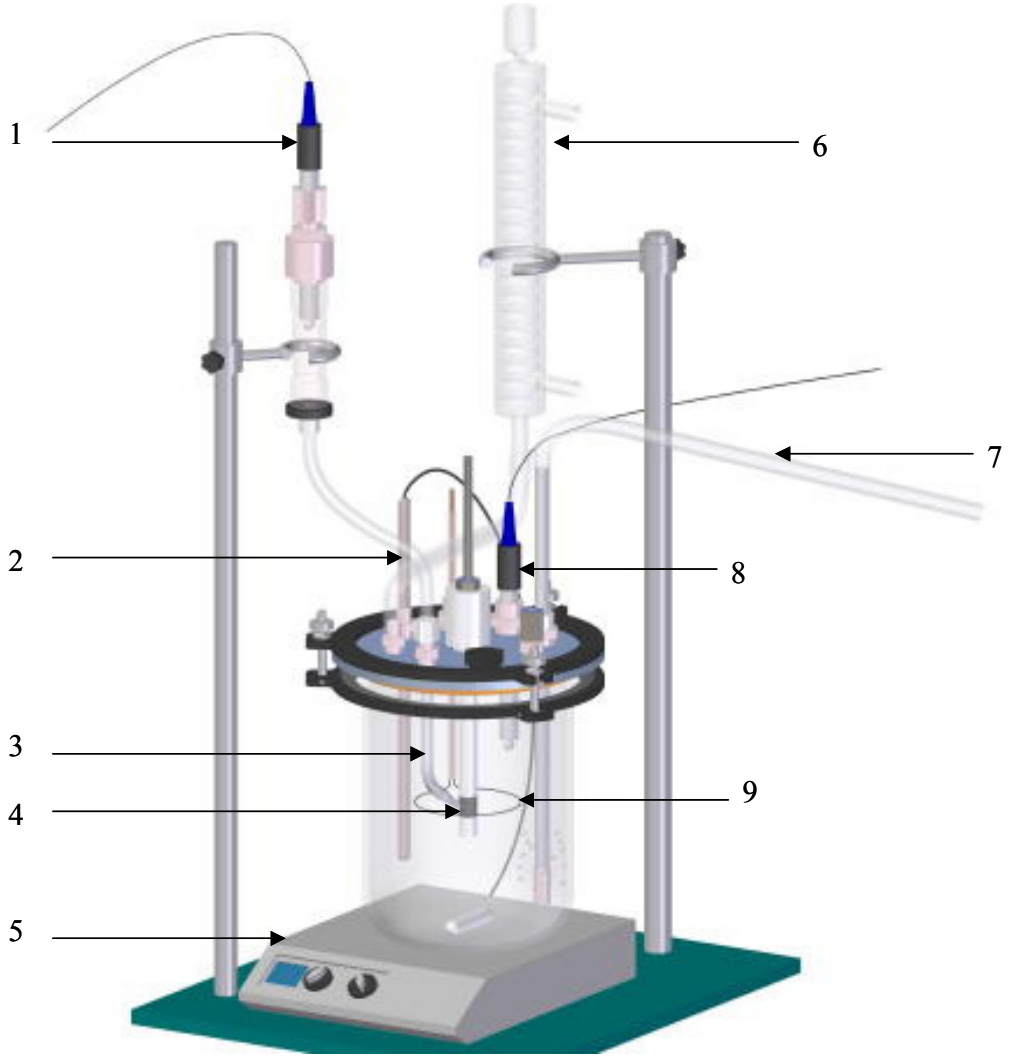

Figure 1. Schematic of a glass cell: 1. reference electrode; 2. temperature probe; 3. luggin capillary; 4. working electrode; 5. hot plate; 6. condenser; 7. bubbler for gas; 8. pH electrode; 9. counter electrode

Electrochemical corrosion measurements were performed by using a potentiostat connected to a PC. Corrosion rates were measured by

using the linear polarization resistance (LPR) method. The coupon with the iron carbonate scale was observed after the experiments by using Scanning Electron Microscopy (SEM). The chemical composition of the X-65 steel used for all the experiments is shown in Table 1. Two types of generic inhibitors were used for the experiments (Table 2and Table 3).

Table 1. Chemical Composition of X65 (wt.%) (Fe is in balance).

C	Mn	Si	P	S	Cr	Cu	Ni	Mo	Al
0.050	1.32	0.31	0.013	0.002	0.042	0.019	0.039	0.031	0.0032

Table 2. Formulation of inhibitor A

Compound	Composition (by weight)
Isopropyl alcohol	35%
Water	35%
Imidazoline acetate salts	30%

Table 3. Formulation of inhibitor B

Compound	Composition (by weight)
Methanol	25%
Water	25%
Imidazoline acetate salts	25%
Benzyl dimethyl coco-quat chloride	25%

Results

The results obtained are presented below in the following manner:

- Experiments with iron carbonate scale formation done at different supersaturations without an inhibitor;
- Experiments done with only inhibitors without any scale;
- Experiments with scale and with addition of inhibitors;
- Modeling of inhibitor-scale interactions.

Baseline iron carbonate precipitation experiments at different supersaturations without inhibitor

This set of experiments was designed to observe the effect of iron carbonate scale formation on corrosion rate at various supersaturations. Supersaturation4 of iron carbonate is defined as:

$$SS = \frac{c_{Fe^{2+}} c_{CO_3^{2-}}}{K_{sp}}$$

The supersaturations were varied from 7 to 150 by varying the pH from 6.0 – 6.6 and the Fe^{2+} concentration from 10 – 50ppm. Table 4 shows the conditions under which these supersaturations were obtained. The effect of change in supersaturation on the corrosion rate is shown in Figure 2. Clearly with higher supersaturation the iron carbonate scale formed faster and the corrosion rate decreased more rapidly. Error bars display the maximum and minimum values obtained in repeated experiments. Increase in the precipitation rate of iron carbonate is also observed in the Figure 2, due to the increase in supersaturation of the solution with respect to iron carbonate. This increase in the precipitation rate results in a decrease in the corrosion rate of the metal, since the scale blocks a part of the steel surface preventing it from corroding, and acts as a diffusion barrier for the corrosive species.

Table 4. Bulk supersaturation of the solution at various pH and Fe^{2+} concentration

pH	Fe^{2+} concentration / ppm	Supersaturation
6.00	50	9
6.30	10	7
6.30	50	37
6.60	10	30
6.60	50	150

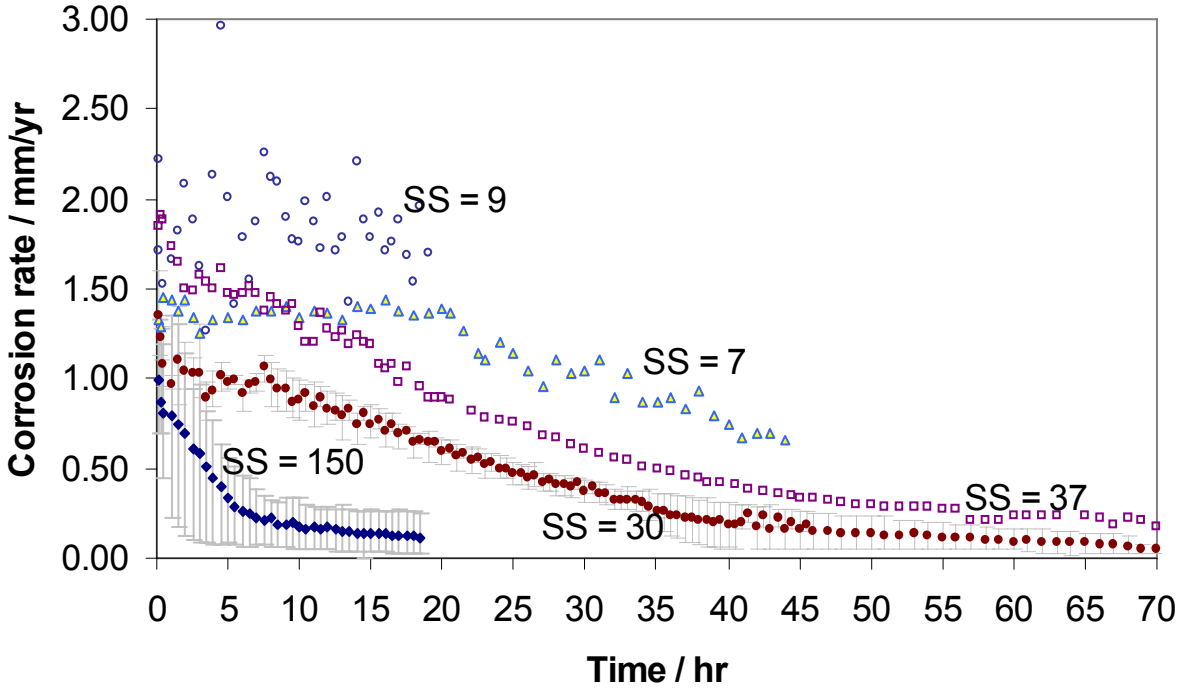

Figure 2. Effect of supersaturation SS on corrosion rate at T = 80°C, no inhibitor, stagnant conditions. Error bars represent minimum and maximum values obtained in repeated experiments.

The top view and the cross-sectional view of the samples at various supersaturations are shown in the Figure 3 – Figure 6. A comparison of scale thickness, crystal grain size, and final corrosion rate for all the baseline experiments at supersaturation of 7 – 150, are shown in Table 5. It is observed that as the supersaturation is increased, the size of the iron carbonate crystals decreases. This is expected since with higher supersaturation and precipitation rates, higher number of crystals nucleate on the surface of the metal. This close proximity of nuclei causes interference in growth of the crystals. It should be noted that at supersaturation of 7, this phenomenon is not observed because the experiment was stopped after 45 hours and the crystals were not allowed to grow any further.

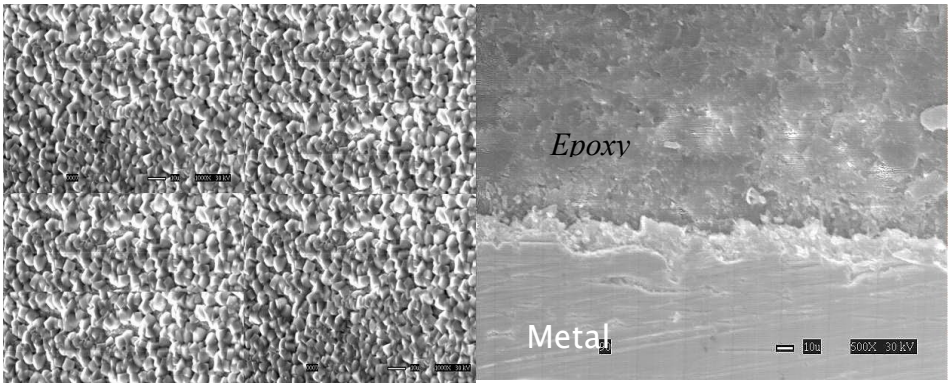

(a) (b)

Figure 3. Top view (a) and cross-sectional view (b) of the sample at 500X, for pH 6.60, Fe^{2+} = 50ppm, no inhibitor, SS = 150, T = 80°C, stagnant conditions.

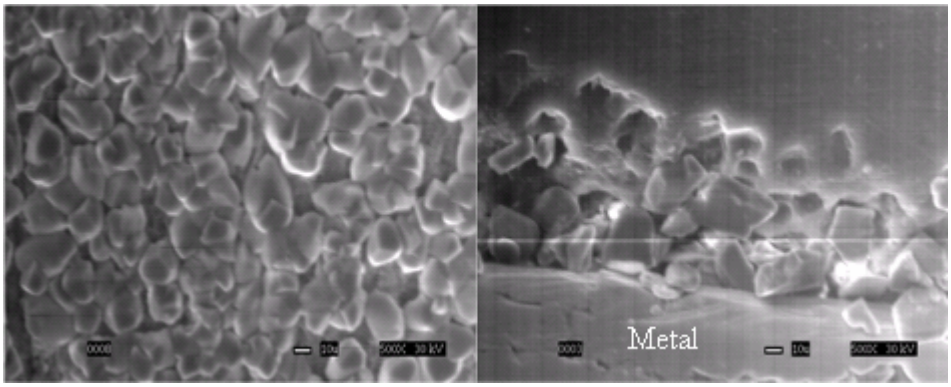

(a) (b)

Figure 4. Top view (a) and cross-sectional view (b) of the sample at 500X, for pH 6.60, Fe^{2+} = 10ppm, no inhibitor, SS = 30, T = 80°C, stagnant conditions.

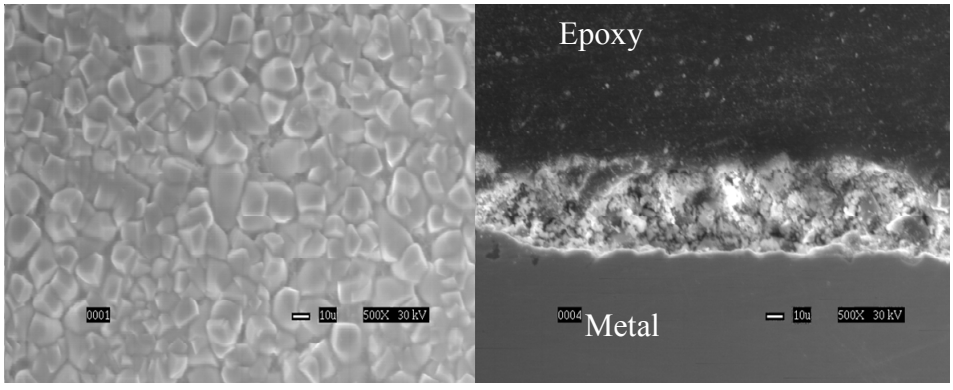

(a) (b)

Figure 5. Top view (a) and the cross-sectional view (b) of the sample at 500X, for pH 6.30, Fe^{2+} = 50ppm, SS = 37, T = 80°C, no inhibitor, stagnant conditions.

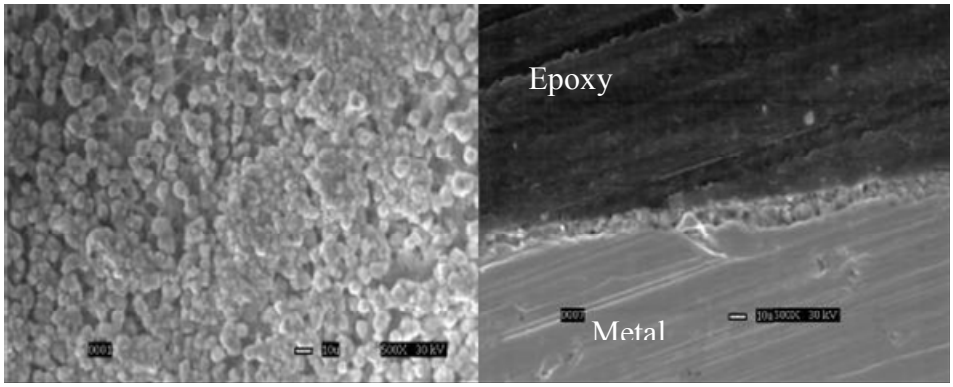

(a) (b)

Figure 6. Top view (a) and the cross-sectional view (b) of the sample at 500X, for pH 6.30, Fe^{2+} = 10ppm, SS = 7, T = 80°C, no inhibitor, stagnant conditions.

Table 5. Summary of baseline experiments at supersaturations of 7 – 150, T = 80°C, no inhibitor, stagnant solutions

SS	t / hr	Thickness / μm	Crystal size / μm	Final corrosion rate / mm/yr
7	45	10	10	0.65
9	19	No scale	No scale	1.8
30	85	30-40	15-25	0.027
37	87	30-40	15-25	0.13
150	19	15-25	5	0.1

Baseline experiments done with only inhibitor and without iron carbonate scale

This set of experiments was designed to study the effect of inhibitor concentration on the corrosion rate under non-scaling conditions.

1. Inhibitor A

The effect of inhibitor A concentration on the corrosion rate is shown in Figure 7. From the figure, it can be seen that at 25ppm the inhibitor is partially protective, while it decreases the corrosion rate by more than 80% at 50ppm. From the potentiodynamic sweeps (Figure 8), the average values of the Tafel slopes were measured to be βa = 62 mV/decade, βc = 98 mV/decade and the 'B' value was calculated to be 16.4 mV. From the sweeps, it can be seen that the inhibitor slows down the anodic reaction as well as the cathodic reaction.

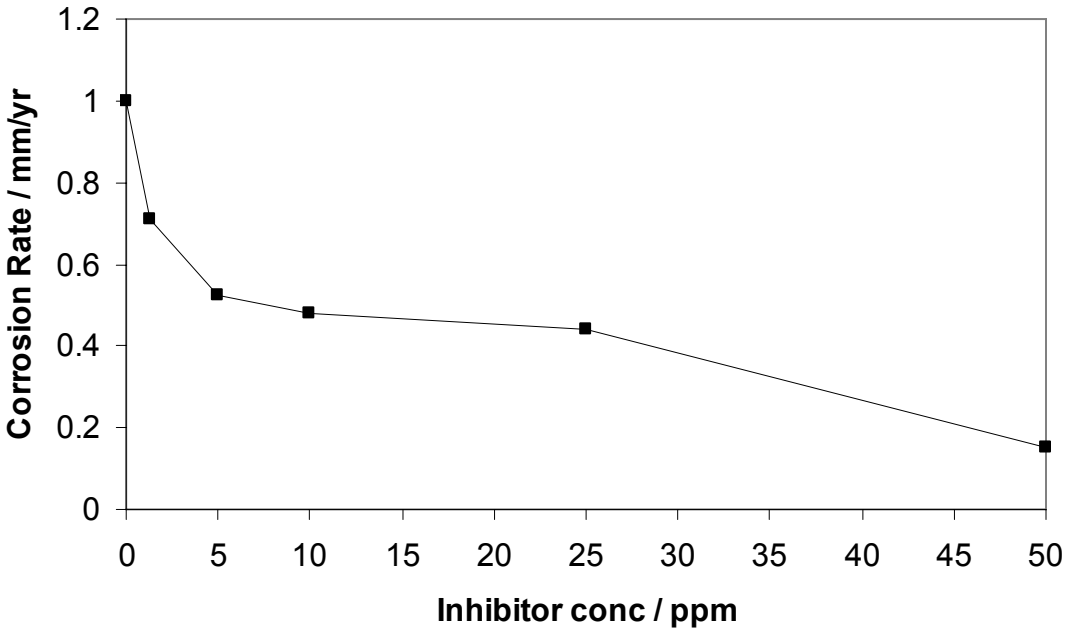

Figure 7. Effect of inhibitor A concentration on the corrosion rate for pH 6.6, T = 80°C, no Fe^{2+} added, stagnant conditions.

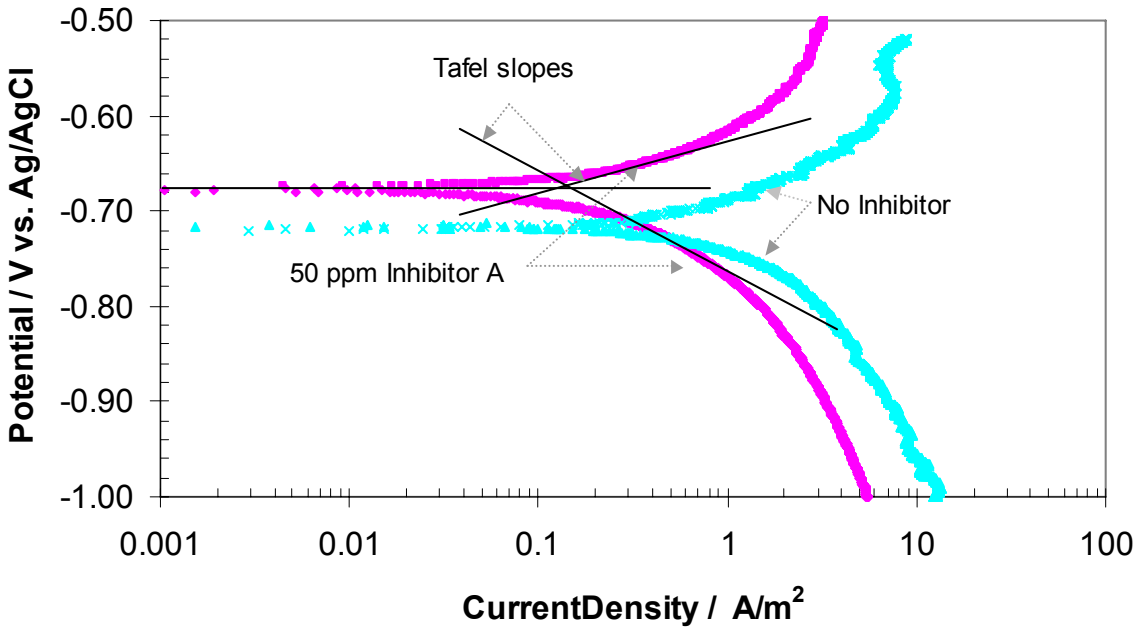

Figure 8. Polarization curves for 50ppm inhibitor A at pH 6.6, T = 80°C, no Fe^{2+} added, stagnant conditions.

2. Inhibitor B

The effect of inhibitor B concentration on the corrosion rate is shown in Figure 9. To study the nature of the inhibitor, the potentiodynamic

sweeps for the experiments were done at pH 6.60. The sweeps were done in the cathodic direction initially. Then after waiting for sometime for the potential to stabilize the anodic sweep was carried out. From the sweeps (Figure 10), the average anodic and the cathodic Tafel slopes for inhibitor B were calculated to be 60 mV/decade and 120 mV/decade respectively and the 'B' value was calculated to be 17.4 mV. Hence, an average 'B' value of 17 mV was used to obtain the corrosion rate from LPR in all the experiments.

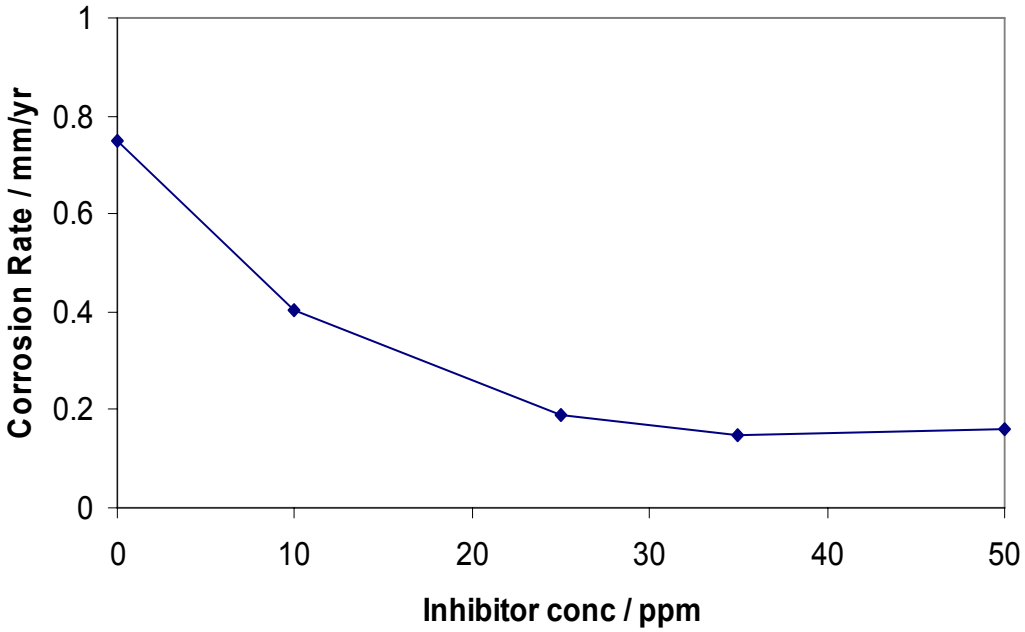

Figure 9. Effect of inhibitor B concentration on the corrosion rate between pH 6.0–6.6, T = 80°C, no Fe^{2+} added, stagnant conditions.

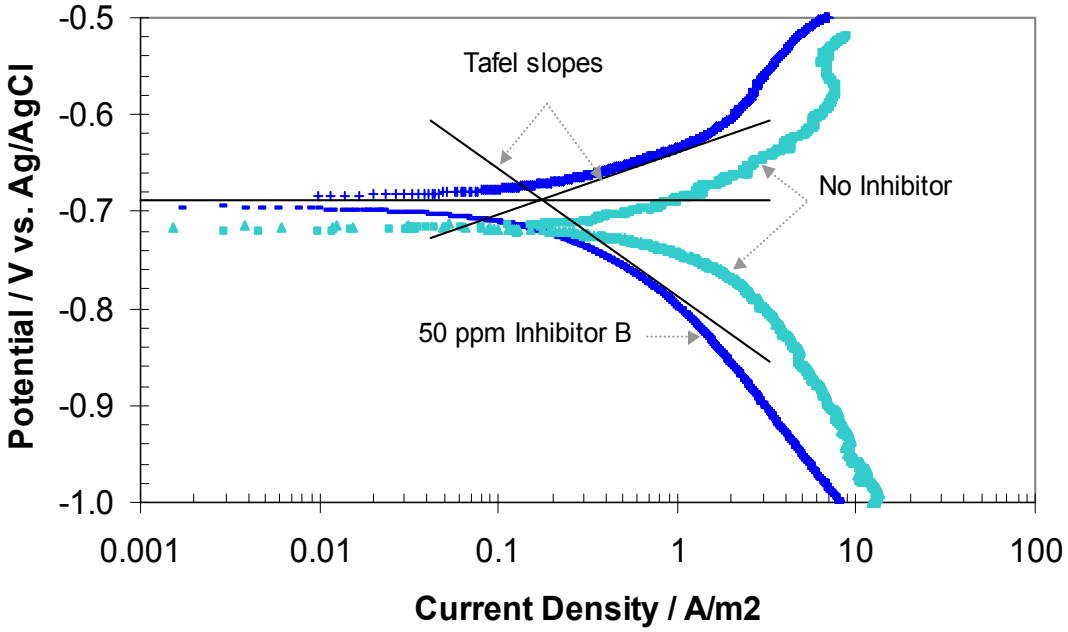

Figure 10. Polarization curves for 50ppm inhibitor B showing the tafel slopes, at pH 6.6, T = 80°C, no Fe^{2+} added, stagnant conditions.

Inhibitor-scale interactions at supersaturation of 150

In this set of experiments a selected concentration of inhibitor A was added to the solution which was at an initial supersaturation of 150 w.r.t. iron carbonate. From Figure 7, it can be seen that at 25ppm, inhibitor A is partially protective. Therefore 25ppm inhibitor was chosen as the concentration to start the testing. In order to study the effect of stronger inhibition, 50ppm inhibitor was added in subsequent experiments.

1. Simultaneous inhibition and scaling

These experiments were designed to see the interaction of the inhibitor and the iron carbonate scale when both species would compete for a place on the metal surface. In the experiment, a supersaturation of 150 was achieved in the beginning of the experiments by adjusting the pH to 6.60 and adding 50ppm of Fe^{2+}. The required amounts of inhibitor A was added after 15 minutes of starting the experiment. On addition of 25ppm of inhibitor A, no effect was seen on the corrosion rate nor on the scale formation, i.e. the scale formation dominated the corrosion process.

However, on addition of 50ppm of inhibitor A, it can be seen that the corrosion rate was reduced to 0.2 mm/yr in less than two hours (Figure 11). However, the final corrosion rate is the same as that without the inhibitor. It can be observed that for this experiment the inhibitor "dominates" the corrosion rate when compared to the iron carbonate scale. From the front view of the sample (Figure 12), it can be seen that very little iron carbonate is seen on the surface of the metal. Therefore, it is confirmed that the metal surface was mainly protected due to the presence of the inhibitor and 50ppm of the inhibitor seemed to have hampered the growth of iron carbonate on the surface of the metal.

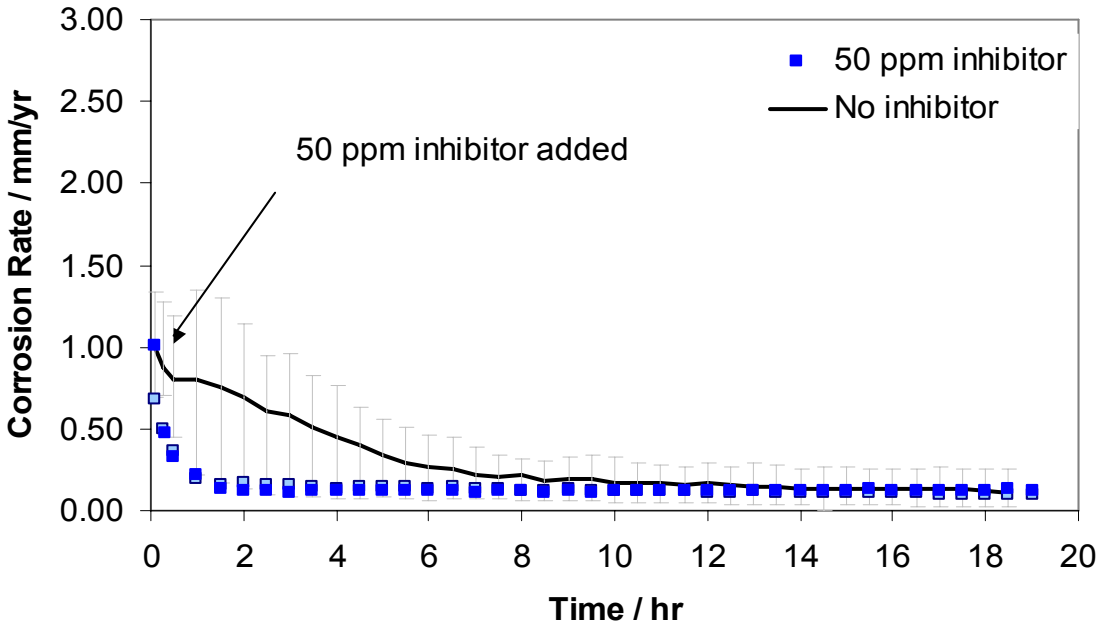

Figure 11. Effect of addition of 50ppm inhibitor A (added initially) on the corrosion rate for pH 6.60, Fe^{2+} = 50ppm, SS = 150, T = 80°C, stagnant conditions.

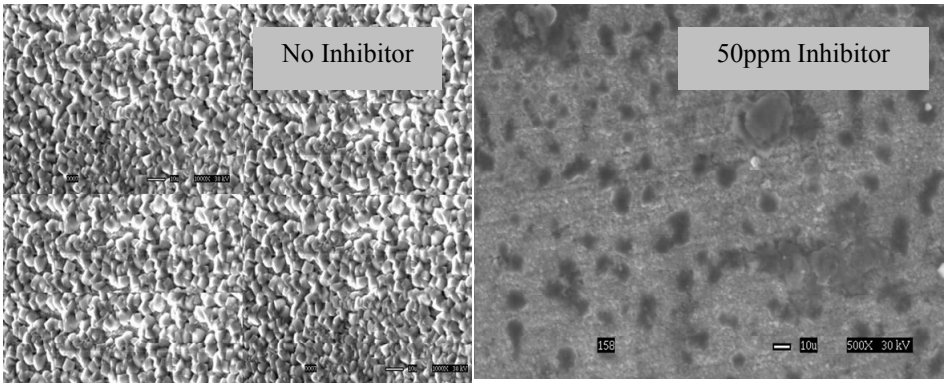

Figure 12. Comparison of top view for specimen at 500X with 50ppm inhibitor A and without inhibitor at pH 6.60, Fe^{2+} = 50ppm, SS = 150, T = 80°C, stagnant conditions.

2. Inhibition of a scaled surface

In this set of experiments, the inhibitor was added after 5 hours. These experiments were designed to see the interaction of the inhibitor and the iron carbonate scale when the latter is partially formed. A supersaturation of 150 was achieved in the beginning by adjusting pH to 6.60 and adding 50ppm of Fe^{2+}. Inhibitor A was added after 5 hours. It is observed that 25ppm of inhibitor had no effect on the corrosion rate nor the scale formation.

Figure 13 shows an experiment in which 50ppm inhibitor was added 5 hours after starting the experiment. In this experiment, it can be seen that as soon as the inhibitor is added, the corrosion rate decreases rapidly. From the top view of the specimen in Figure 14, it is seen that there are only a few crystals of iron carbonate formed on the surface of the metal. These iron carbonate crystals probably formed before the addition of the inhibitor and hence it is concluded that the inhibitor hampered the growth of the iron carbonate scale.

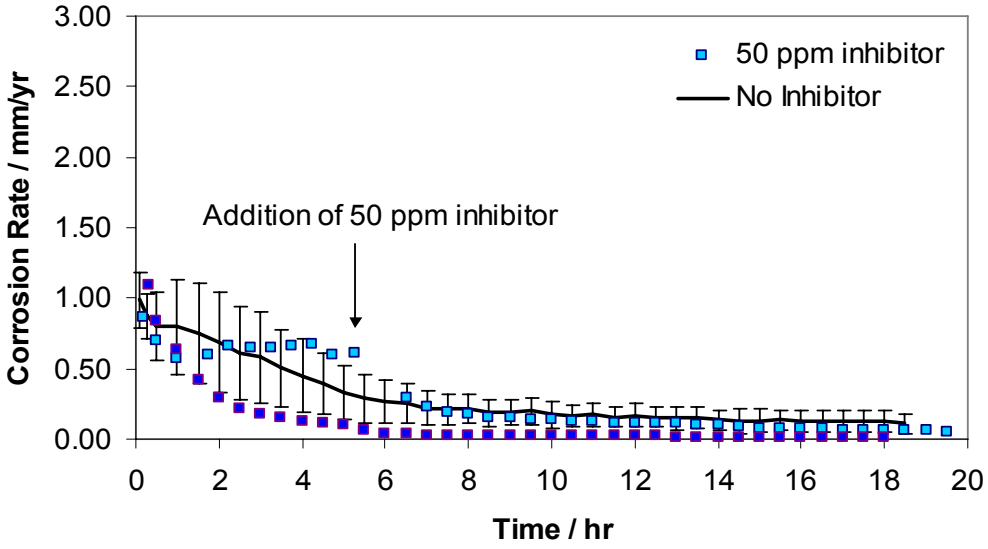

Figure 13. Effect of addition of 50 ppm inhibitor A after 5 hours on corrosion rate for pH 6.60, Fe^{2+} = 50ppm, SS = 150, T = 80°C, stagnant conditions.

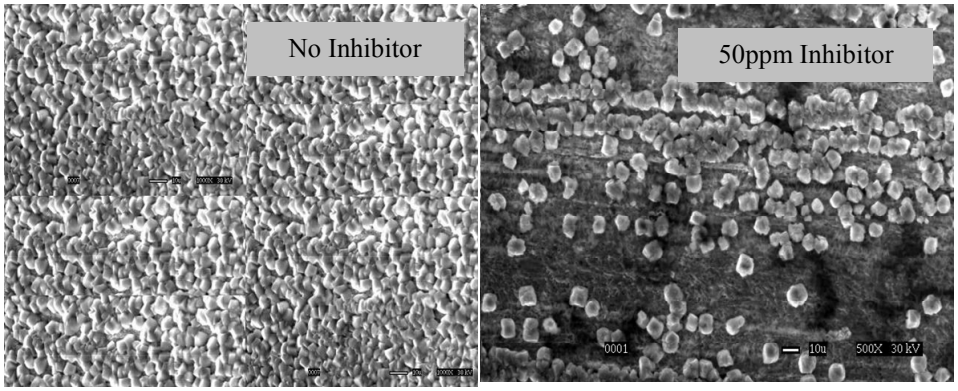

Figure 14. Comparison of top view for specimen at 500X with 50ppm inhibitor A added after 5 hours and without inhibitor at pH 6.60, Fe^{2+} = 50ppm, SS = 150, T = 80°C, stagnant conditions.

Inhibitor-scale interactions at supersaturation of 30

The supersaturation of the solution was lowered to test the inhibitor scale interaction under lower iron carbonate precipitation rates. In this set of experiments, 25ppm of inhibitor B is added to the solution that is at an initial supersaturation of 30. Since a possible antagonistic interaction between the inhibitor and the scale was sought, a low concentration of the inhibitor which was only partially protective was

chosen. From Figure 9, it is seen that 25ppm of inhibitor B fit our criteria very well.

1. Simultaneous inhibition and scaling

These experiments were designed to see the interaction of the inhibitor and the iron carbonate scale when both the processes would compete for a place on the metal surface. In the experiment shown in Figure 15, a supersaturation of 30 was achieved in the beginning by adjusting pH to 6.60 and adding 10ppm of Fe^{2+}. Subsequently 25ppm inhibitor B was added after 30 minutes. The figure shows the comparison between the experiments with

- Only 25ppm inhibitor B
- Only iron carbonate scale
- 25ppm inhibitor added under scaling conditions.

It can be found that when 25ppm inhibitor is added under scaling conditions, the decrease in the corrosion rate is faster than seen in the other two conditions. However, from the logarithmic graph of the above experiment (Figure 16), it is noticed that the final corrosion rate is similar to that without the inhibitor.

From the top view of the sample (Figure 17), very little iron carbonate is observed on the surface of the metal. Therefore, it seems that the metal surface is mainly protected due to the presence of the inhibitor. Adding 25ppm of inhibitor B seems to hamper the growth of iron carbonate on the surface of the metal.

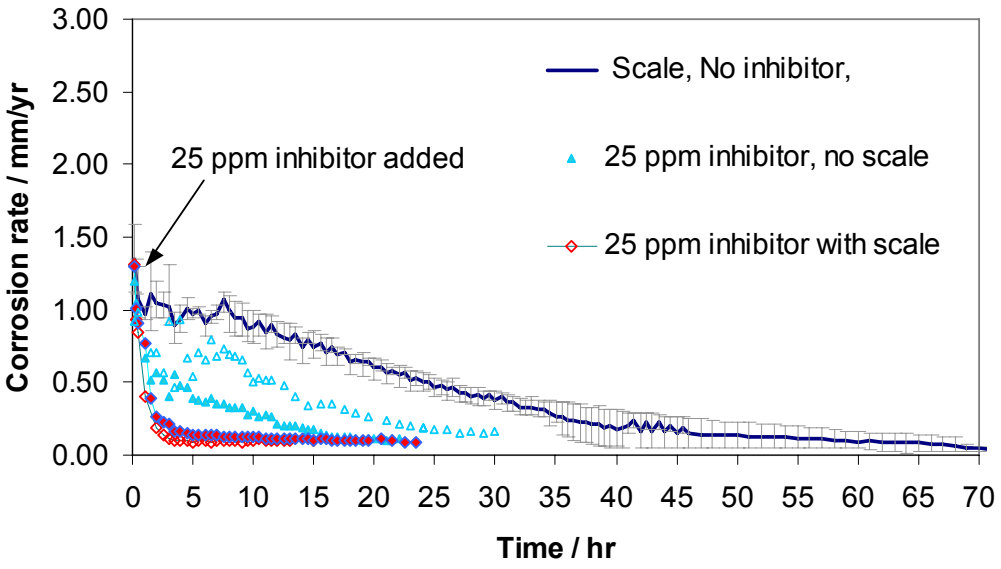

Figure 15. Effect of addition of 25 ppm inhibitor B added after 0.5 hr. on corrosion rate for pH 6.60, Fe^{2+} = 10ppm, SS = 30, T = 80°C , stagnant conditions. Same symbol shapes depict repetitions of the same experiments.

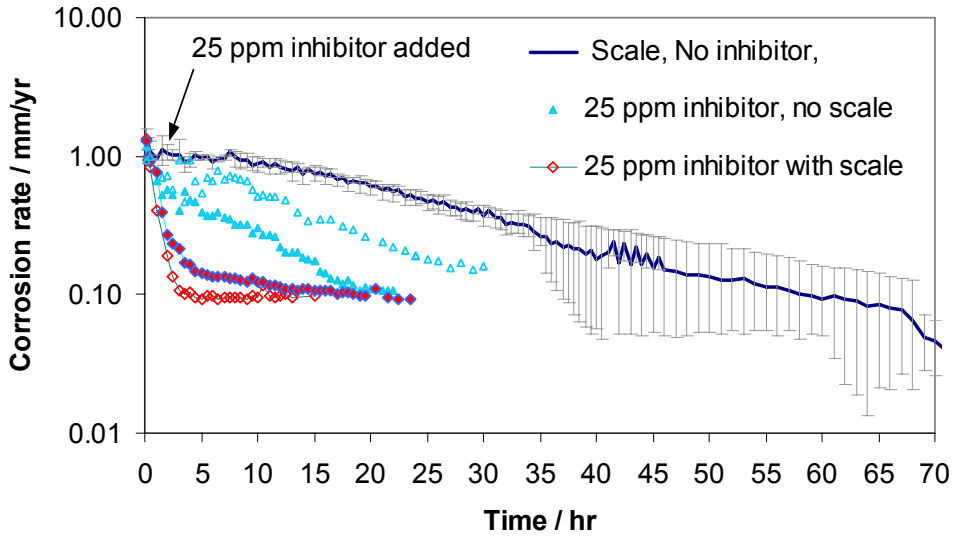

Figure 16. Effect of addition of 25ppm inhibitor B added after 0.5 hr. on corrosion rate for pH 6.60, Fe^{2+} = 10ppm, SS = 30, T = 80°C , stagnant conditions. Same symbol shapes depict repetitions of the same experiments.

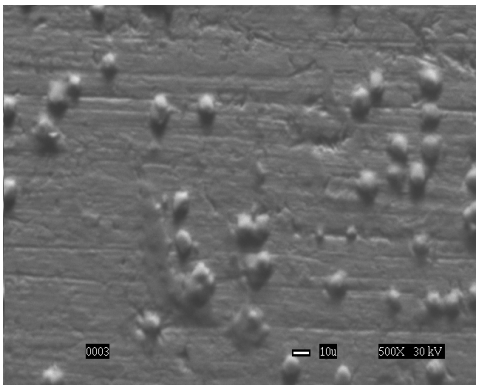

Figure 17. The top view of sample at 500X when 25ppm inhibitor B is added after 0.5 hr for pH 6.60, Fe^{2+} = 10ppm, SS = 30, T = 80^{o}C, stagnant conditions.

2. Inhibition of a scaled surface

In these set of experiments, 25ppm of inhibitor was added after 35 – 40 hours of starting the experiment that was at an initial supersaturation of 30. Comparison of the experiments with and without inhibitor is shown in Figure 18. It is seen that as soon as the inhibitor is added, the corrosion rate decreases drastically. However, from the logarithmic graph of the same experiment (Figure 19), it is noticed that the final corrosion rate remains similar. From the top and the cross-sectional view of the sample (Figure 20), a porous iron carbonate scale of thickness 10 μm is observed.

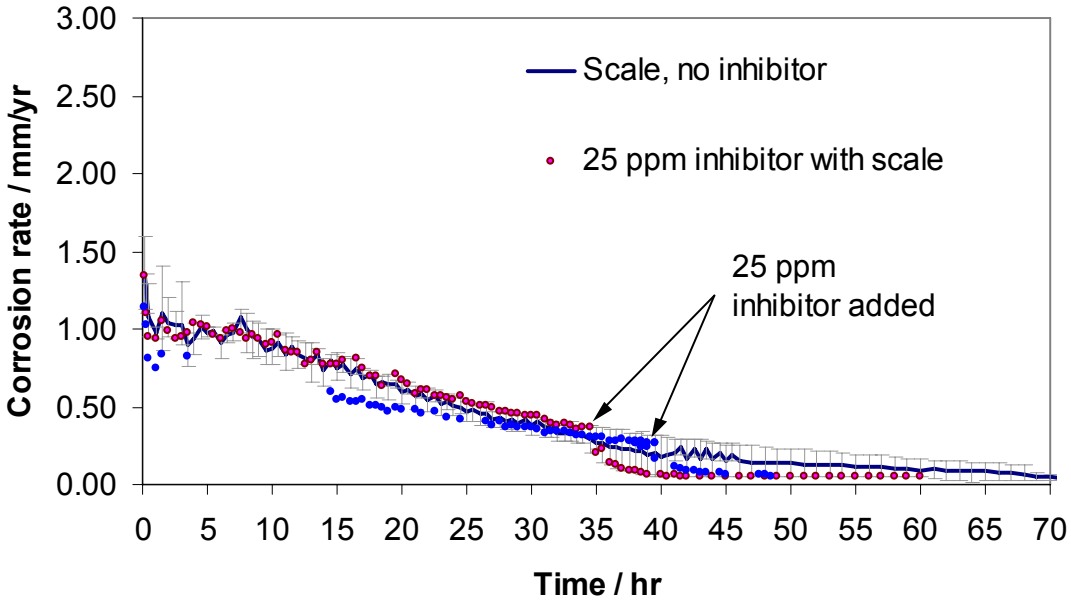

Figure 18. Effect of addition of 25ppm inhibitor B added after 35 hr. on corrosion rate for pH 6.60, Fe^{2+} = 10ppm, SS = 30, T = 80°C, stagnant conditions.

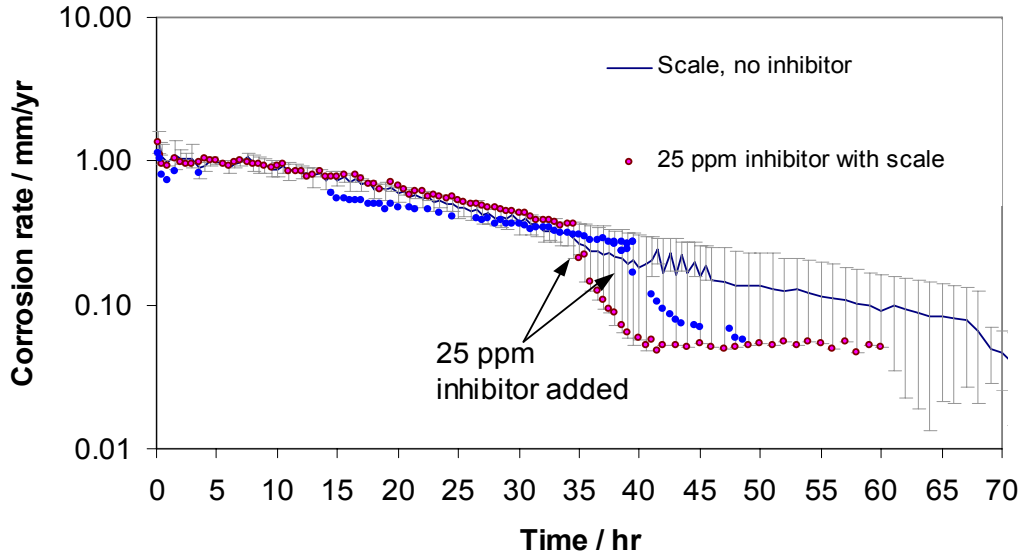

Figure 19. Effect of addition of 25ppm inhibitor B added after 35 hr. on corrosion rate for pH 6.60, Fe^{2+} = 10ppm, SS = 30, T = 80°C, stagnant conditions.

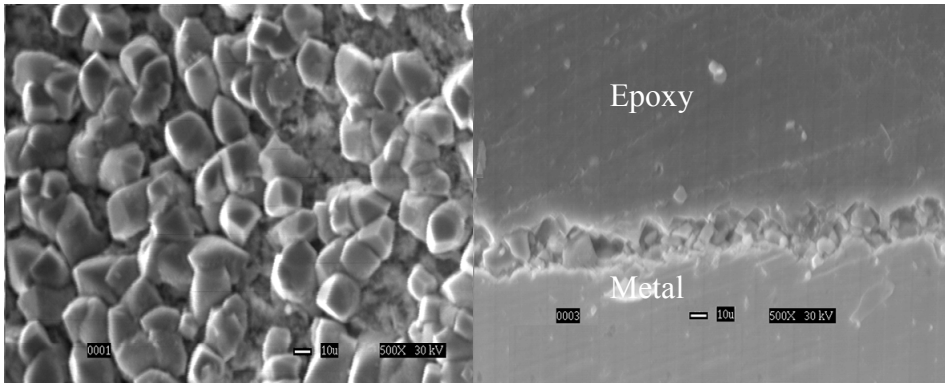

(a) (b)

Figure 20. The top view (a) and the cross-sectional view (b) of sample at 500X when 25ppm inhibitor B is added after 35 hr for pH 6.60, Fe^{2+} = 10ppm, SS = 30, T = 80°C, stagnant conditions.

Inhibitor-scale Interactions at supersaturation of 7

Experiments at supersaturation of 7 were done to test the inhibitor-scale interaction at an even slower iron carbonate precipitation rate. In this experiment, the inhibitor was added after creating a very porous iron carbonate scale (Figure 6). Supersaturation of 7 was achieved in the beginning by adjusting the pH to 6.30 and adding 10ppm of Fe^{2+}. Subsequently, 25ppm inhibitor B was added after 47 hours. From the comparison of the experiments with and without inhibitor (Figure 21), it is seen that as soon as the inhibitor is added, the corrosion rate decreases and no antagonistic behavior is observed. By looking at the scale (Figure 22), it was found that the porosity of the scale was very similar to that without the inhibitor.

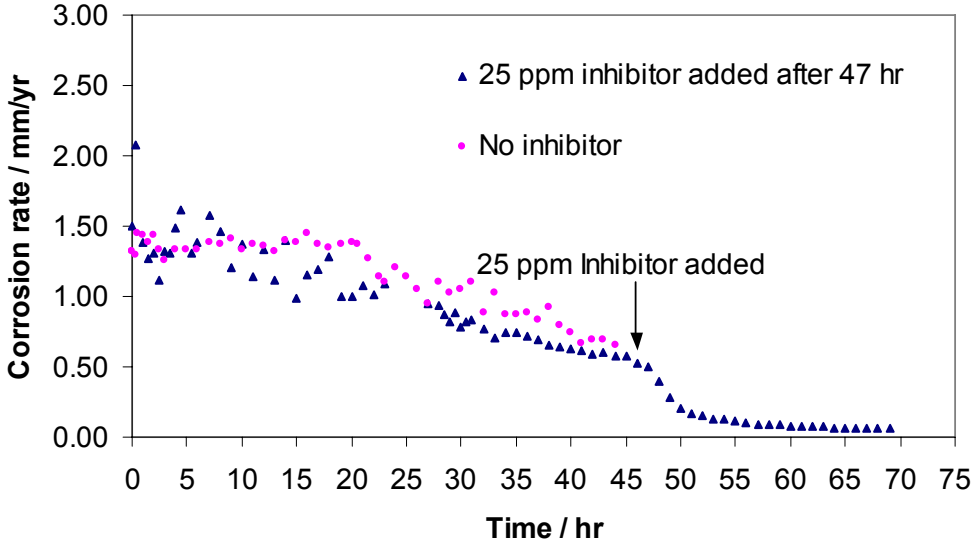

Figure 21.Change in corrosion rate with time when inhibitor B is added after 47 hours, at pH 6.30, Fe^{2+} = 10ppm, SS = 7, T = 80°C, stagnant conditions.

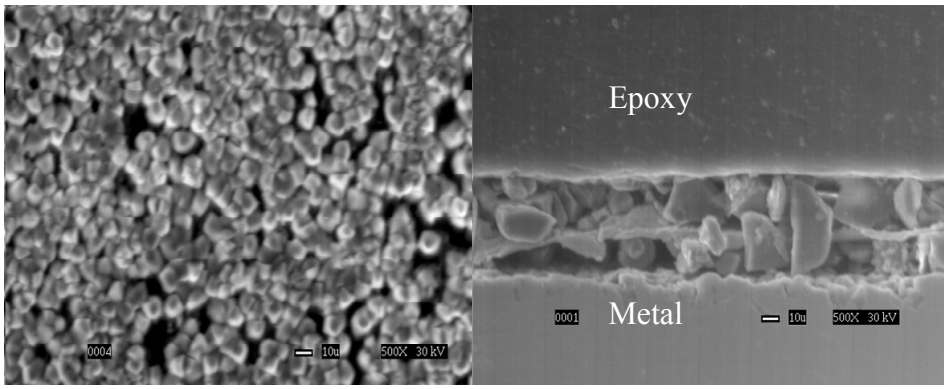

(a) (b)

Figure 22. The top view (a) and the cross-sectional view (b) of sample at 500X when 25 ppm inhibitor B is added after 47 hr. for pH 6.30, Fe^{2+} = 10ppm, SS = 7, T = 80°C, stagnant conditions.

Modeling of inhibitor-scale interaction

From the experimental results it was observed that the protective effects of the corrosion inhibitor and the scale were complementary and no antagonism was observed. However, some interference was seen: the presence of inhibitors hampered the growth of iron

carbonate scale. This was initially attributed to the scale growth inhibition properties of the corrosion inhibitor. Upon a more in-depth analysis it was found that the concentration of Fe^{2+} on the surface of the steel i.e. the surface supersaturation could be one of the major factors affecting scale formation. This analysis is explained in the following paragraphs.

Normally the sources of ferrous ions that contribute to the precipitation of iron carbonate are the bulk solution as well as the corroding steel surface. In the presence of the inhibitors, the corrosion rate of the metal decreases and the diffusion of Fe^{2+} from the bulk solution remains the only source of ions for precipitation at the metal surface. Since, the kinetics of precipitation of the iron carbonate may be faster than the rate of transport of Fe^{2+} from the bulk of the solution to the surface, the precipitation becomes diffusion-controlled and slows down.

The above phenomenon can be simulated using Ohio University's MULTICORP V3.0 software package. The model was run under the following conditions: pH 6.60, Fe^{2+} concentration of 50ppm, SS = 150, T = 80^{o}C. One simulation was run with an inhibitor (assuming 99% efficiency) and another without the inhibitor. It is seen that in the presence of the inhibitor the Fe^{2+} concentration (Figure 23) as well as the pH (Figure 24) near the surface of the metal is lower than that in the absence of the inhibitor. This leads to a lower supersaturation and a slower precipitation rate near the metal surface when the inhibitor is added. From the comparison of the scales obtained using the model (Figure 25), it is seen that the thickness of the iron carbonate scale formed in the presence of the inhibitor is approximately five times less when compared to the scale thickness formed in the absence of the inhibitor.

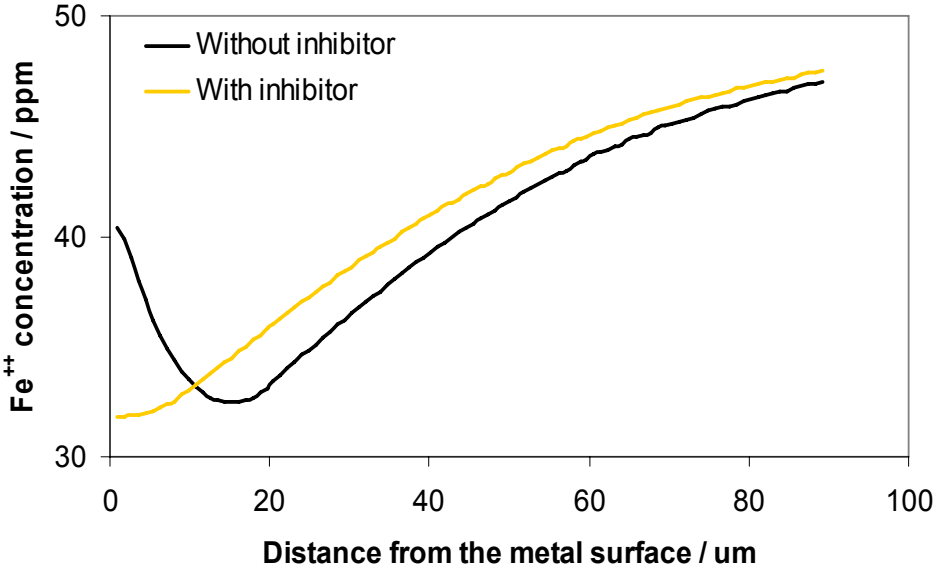

Figure 23. Fe2+ concentration profile with and without the inhibitor obtained using MULTICORP 3.0 at pH 6.60, Fe^{2+} = 50ppm, SS = 150, T = 80°C.

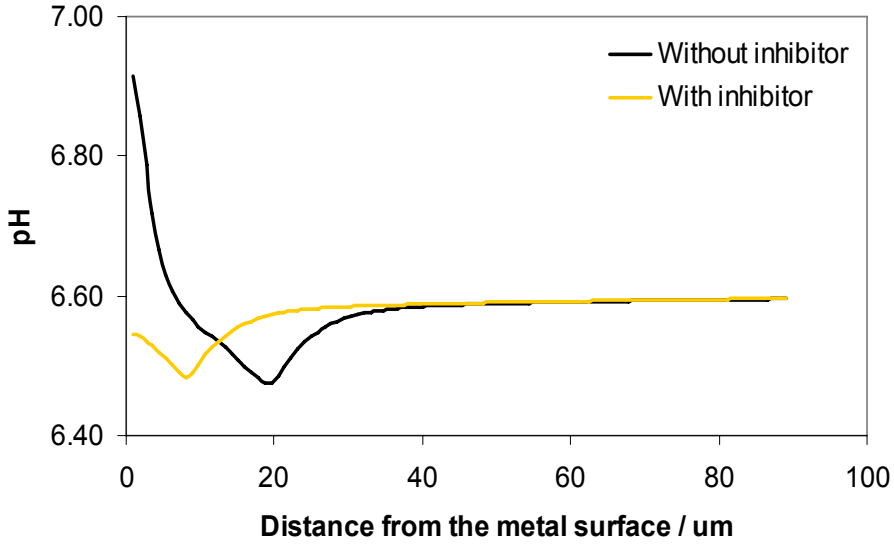

Figure 24. pH profile with and without the inhibitor obtained using MULTICORP 3.0 at pH 6.60, Fe^{2+} = 50ppm, SS = 150, T = 80°C.

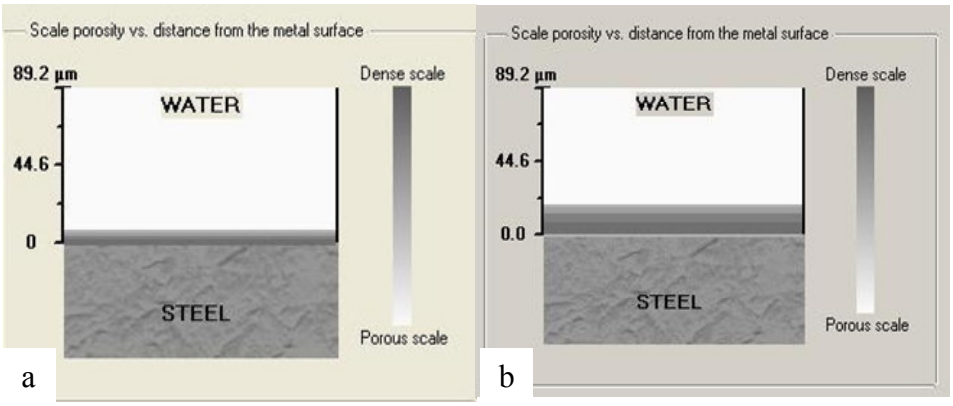

Figure 25. Comparison of the iron carbonate scale obtained (a) with and (b) without inhibitor using MULTICORP 3.0 at pH 6.60, Fe^{2+} = 50ppm, T = 80°C.

Hence, in the absence of corroding conditions at the metal surface, there would be less scale formed at the steel surface. Similar phenomenon was also observed in a series of experiments on stainless steel. At a supersaturation of 30, it was found that even after 3 days no iron carbonate scale was formed on the surface of steel. In an experiment done at supersaturation of 150, scale precipitated on stainless steel was approximately 50% of that compared to corroding mild steel.

From the above analysis, it is deduced that the lower concentration of Fe^{2+} at the metal surface might be the primary reason the growth of scale is hampered in the presence of inhibitor. In addition, the scale growth inhibition properties of the inhibitor could play a role, however no direct evidence for this was found.

Iron carbonate scale precipitation and the interaction between the inhibitor film and the iron carbonate scale have been studied. The interaction was tested using various concentrations of two imidazoline-based generic inhibitors in the iron carbonate supersaturation range of 7 – 150. Based on the experimental conditions, the main research findings are:

The generic corrosion inhibitors used in this study worked by slowing down anodic as well as cathodic reactions.

Above a certain threshold concentration, both inhibitors hampered the growth of the iron carbonate scale. This could be a result of a

decreased concentration of Fe^{2+} at the surface of the steel and/or scale growth inhibition properties of the corrosion inhibitor.

No conditions were found under which inhibitor and scale interacted in an antagonistic manner. i.e. in all of the conditions investigated, the combination of inhibitor and iron carbonate scale never failed to reduce the corrosion rate.

Conclusions

Iron carbonate scale precipitation and the interaction between the inhibitor film and the iron carbonate scale have been studied. The interaction was tested using various concentrations of two imidazoline-based generic inhibitors in the iron carbonate supersaturation range of 7 – 150. Based on the experimental conditions, the main research findings are:

- The generic corrosion inhibitors used in this study worked by slowing down anodic as well as cathodic reactions.
- Above a certain threshold concentration, both inhibitors hampered the growth of the iron carbonate scale. This could be a result of a decreased concentration of Fe^{2+} at the surface of the steel and/or scale growth inhibition properties of the corrosion inhibitor.
- No conditions were found under which inhibitor and scale interacted in an antagonistic manner. i.e. in all of the conditions investigated, the combination of inhibitor and iron carbonate scale never failed to reduce the corrosion rate

Acknowledgments

The authors acknowledge all the companies who give the financial support and technical directions. They are BP, Champion Technologies, ChevronTexco, Clariant TR Oil Services, Conocophillips, Dynea, Eni, ExxonMobil, ONDEO Nalco, Petrobras, Saudi Aramco, Shell, and Total.

References

1. M. B. Kermani and A. Morshed, *Corrosion, 59*, 659(2003).

2. P. Roberge, *Handbook of corrosion engineering*, McGraw Hill, (1999).

3. E. Gulbrandsen, S. Nesic, A. Stangeland, T Buchardt, B. Sundfaer, S. M. Hesjevik, and S. Skjerve, *Corrosion/98*, paper no. 013, Houston, NACE International, (1998).

4. A. Ikeda, M. Ueda, and S. Mukai, *Advances in CO_2 Corrosion*, 1, 52, Houston, NACE International, (1984).

5. M. L. Johnson and M. B. Tomson, *Corrosion/91*, paper no. 268, Houston, NACE International (1991).

6. A. Dugstad, *Corrosion/92*, paper no. 14, Houston, NACE International (1992).

7. A. Dugstad, L. Lunde, and K. Videm, *Corrosion/94*, paper no. 14, Houston, NACE International (1994).

8. E. W. J. van Hunnik, B. F. M. Pots, and E. L. J. A. Hendriksen, *Corrosion/96*, paper no. 6, Houston, NACE International (1996).

9. S. Nesic, M. Nordsveen, R. Nyborg, and A. Stangeland, *Corrosion/2001*, paper no. 01040, Houston, NACE International (2001).

10. S. Nesic and K.-L. J. Lee, *Corrosion*, 59, 616 (2003).

11. V. J. Drazic and D. M. Drazic, *Proc. 7th European Symposium on Corrosion Inhibitors (7SEIC)*, Ann. Univ. Ferrara, N.S., Sez. V, Suppl. N. 9, 1990, Ferrara, p.99 (1990).

12. S. Nesic, W. Wilhelmsen, S. Skjerve, and S. M. Hesjevik, *Proceedings of the 8th European Symposium on Corrosion Inhibitors*, Ann. Univ. Ferrara, N.S., Sez. V, Suppl. N. 10, p.1163 (1995).

13. H. Malik, *Corrosion*, 51, 321 (1995).